

The Search for Pseudogoldstone Bosons at a High Energy Linear Collider*

M. L. Swartz

Stanford Linear Accelerator Center, Stanford University, Stanford, California, 94309

ABSTRACT

A TeV electron-positron collider is a useful device in the search for color singlet and octet pseudo-Nambu-Goldstone bosons (PNGBs). Charged PNGBs can be discovered if their masses are less than $0.45\text{--}0.49\sqrt{s}$. The discovery reach for neutral states depends upon the ratio N_{tc}/F_{tc} . Three of the four neutral states can be discovered if their masses are less than 350-524 GeV even for the conservative parameter choice $N_{tc}/F_{tc} = 3/123$ GeV.

I. INTRODUCTION

All non-minimal models of strongly-coupled electroweak symmetry breaking include a spectrum of technipions. Since they are the pseudo-Nambu-Goldstone bosons (PNGBs) which follow from the spontaneous breaking of a chiral gauge symmetry, the technipions are generally expected to be the lightest technihadrons contained in the theory. They would therefore be the states that are most accessible to experimental observation.

The PNGB spectra of the more realistic models include color singlet, triplet, and octet states which are also singlets and triplets of the residual $SU(2)_V$ symmetry. The color triplet states are leptoquarks and are covered by searches for more generic leptoquarks. The color singlet and octet technipions have less unique decay signatures and are the subject of this document. The standard notation for these states is defined in Table I.

Table I: The quantum numbers of various PNGB states.

$SU(3)_c/SU(2)_V$	1	3
1	$P^{0'}$	P^0, P^\pm
8	$P_8^{0'}$	P_8^0, P_8^\pm

The search for PNGBs at a high energy electron-positron collider has a number of advantages over one performed at a high energy hadron collider. The backgrounds to the various technipion signatures have electroweak cross sections and never overwhelm the signal process. The b-quark tagging in the high energy e^+e^- environment is quite efficient and pure [1] (efficiencies of 60% per b-jet can be obtained with purities of 95%). The large electron beam polarization ($\mathcal{P}_e \simeq 0.8$) improves the separation of the signal and noise and would, in the case of a discovery, help to determine the quantum numbers of the produced state. Finally, the beam energy constraint improves the kinematical separation of the signal and background. All this being said, the technipion mass reach of a high energy e^+e^-

collider is limited to the center-of-mass energy (\sqrt{s}) for neutral states and to $\sqrt{s}/2$ for charged states, and this may be not be adequate to explore the entire parameter space of physically interesting models.

The following two sections of this paper discuss the PNGB search and discovery potential of a high energy e^+e^- collider. The first section reviews the case for the charged states. The second section discusses the case for the neutral states which, until now, has not been studied.

The following sections assume that a 1 TeV collider can produce an integrated luminosity of 100 fb^{-1} in a year or two of operation. This corresponds to approximately 10,000 units of inverse electromagnetic point cross section (the point cross section $\sigma_0 = 4\pi\alpha^2(s)/3s$ is 103.5 fb at 1 TeV).

II. CHARGED PSEUDOGLDOSTONE BOSONS

A. Production Rate

The charged states P^\pm and P_8^\pm have gauge couplings to the photon and Z^0 [2]. If not suppressed kinematically, they are produced copiously in electron-positron collisions. Assuming that form-factor effects are small near threshold, the production cross-section σ^\pm for the charged states is given by the following expression (which assumes $s \gg M_Z^2$),

$$\begin{aligned} \sigma^\pm = & \frac{1}{4} N_c \beta^3 \left\{ 1 + 2 \left[\frac{\cos 2\theta_W}{2 \sin^2 2\theta_W} \right] (c_v + \mathcal{P}_e c_a) \right. \\ & \left. + \left[\frac{\cos 2\theta_W}{2 \sin^2 2\theta_W} \right]^2 (c_v^2 + c_a^2) (1 + \mathcal{P}_e A_e) \right\} \end{aligned} \quad (1)$$

where: the cross section is given in units of the point cross section σ_0 , N_c is the number of final state colors, $\beta = \sqrt{1 - 4M_P^2/s}$ is the velocity of the PNGBs (of mass M_P) in the cm-frame, $c_v = 1 - 4 \sin^2 \theta_W$ is the Z^0 vector coupling to the electron, $c_a = 1$ is the Z^0 axial-vector coupling to the electron, \mathcal{P}_e is the longitudinal polarization of the electron beam in the left-handed basis ($\mathcal{P}_e = 1$ is a purely left-handed beam), and A_e is the left-right Z^0 coupling asymmetry.

Inserting appropriate numbers into equation 1, the cross sections in point cross section units for the color singlet and octet states are,

$$\sigma^\pm = \begin{cases} 0.30\beta^3 & P^\pm \\ 2.40\beta^3 & P_8^\pm, \end{cases} \quad (2)$$

and the left-right asymmetry for charged PNGB production is 0.65. By comparison, the cross section and left-right production asymmetry for the dominant background, the $t\bar{t}$ final state, are about 1.9 point cross section units and 0.34, respectively.

* Work supported by Department of Energy contract DE-AC03-76SF00515

B. Signatures and Backgrounds

In general, the branching ratios of PNGBs are model- and parameter-dependent. If kinematically allowed, the charged PNGBs decay predominantly to the heaviest fermion doublet, $t\bar{b}$ or $\bar{t}b$. The entire decay chain therefore produces four b-quarks and two on-shell W 's in the final state,

$$e^+e^- \rightarrow P^+P^- \rightarrow t\bar{b}\bar{t}b \rightarrow W^+b\bar{b}W^-b\bar{b} \quad (3)$$

The most copious Standard Model background to the P^+P^- signal is the production of $t\bar{t}g^*$ where the off-shell gluon g^* materializes as a massive $b\bar{b}$ pair. This cross section for this process in the relevant kinematic region is less than a percent of the total $t\bar{t}$ cross section.

C. Discovery Limits

The large angular coverage of the calorimetry and tracking system of a future e^+e^- detector will permit the measurement of jets and leptons in the region of polar angle $|\cos\theta| < 0.95$ [3]. The efficiency for the detection of at least 3 tagged, high energy b -jets and 3 additional jets or leptons can be reasonably large (5-10%). It should therefore be possible to discover the color-singlet states with five-sigma significance if the pseudoscalar mass is less than approximately $0.45\sqrt{s}$ and to discover the color-octet states if the mass is less than $0.49\sqrt{s}$.

III. NEUTRAL PSEUDOGOLDSTONE BOSONS

Neutral PNGBs do not have gauge couplings to the photon or Z^0 , but do couple to pairs of gauge bosons via ABJ-type anomaly triangles. It is therefore possible to produce single neutral PNGBs in association with gauge bosons in electron-positron collisions (see Fig. 1). The search for the process $e^+e^- \rightarrow P^0\gamma$ at LEP energies has been studied by several authors [4, 5]. At a high energy e^+e^- collider, several other final states become feasible.

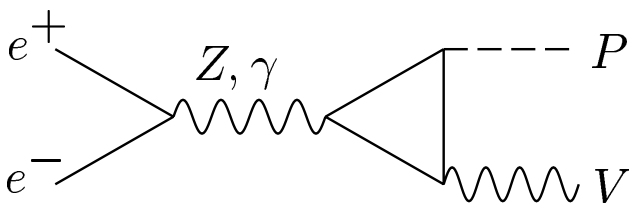


Figure 1: Production of PNGB-gauge boson pairs in an e^+e^- collision.

The amplitude for the Vector-Vector-PNGB coupling is given as follows,

$$\mathcal{A}_{PV_1V_2} = \frac{S_{PV_1V_2}}{8\pi^2\sqrt{2}F_{tc}}\epsilon_{\alpha\beta\gamma\delta}\varepsilon^\alpha(k_1)\varepsilon^\beta(k_2)k_1^\gamma k_2^\delta, \quad (4)$$

where: F_{tc} is the analog pseudoscalar decay constant which is typically 123 GeV (one half of the 246 GeV Higgs field VEV in the Minimal Standard Model) in conservative models of strong EWSB, N_{tc} is the number of technicolors in the model, k_1 and k_2 are the 4-momenta of the vector bosons V_1 and V_2 , $\varepsilon(k_1)$ and $\varepsilon(k_2)$ are the polarizations of the vector bosons and $S_{PV_1V_2}$ is the ABJ anomaly factor [6, 7].

A. Production Rates

The cross sections for the production of various PV final states follow from the coupling given in equation 4. Note that recent calculations of the cross sections [4, 8] correct an error (of a factor of four) in those found in the classical literature [7] for the case $V_1 \neq V_2$. Since the coupling is quadratic in the momenta of the gauge bosons, the cross sections are independent of s in the region $s \gg M_Z^2$ (as s increases well above PNGB threshold, form-factor suppression of the cross section would become significant). In units of point cross section, they increase linearly with s . Since the cross sections for background processes decrease as s^{-1} (constant in point cross section units), the signal-to-noise ratio improves at higher energies. The cross sections are not model-independent but depend upon the square of the ratio N_{tc}/F_{tc} . The largest cross sections are for the production of the P^0g , $P^{0'}g$, $P^0\gamma$, and $P^{0'}\gamma$ final states. They are summarized below (in point cross section units):

$$1. e^+e^- \rightarrow P_s^0g:$$

$$\sigma = \frac{\alpha_s N_{tc}^2}{8\pi^3} \frac{s}{F_{tc}^2} \bar{\beta}^3 \left\{ 1 + 2 \left[\frac{\cot^2 2\theta_W}{2} \right] (c_v + \mathcal{P}_e c_a) + \left[\frac{\cot^2 2\theta_W}{2} \right]^2 (c_v^2 + c_a^2) (1 + \mathcal{P}_e A_e) \right\} \quad (5)$$

$$2. e^+e^- \rightarrow P_s^{0'}g:$$

$$\sigma = \frac{\alpha_s N_{tc}^2}{72\pi^3} \frac{s}{F_{tc}^2} \bar{\beta}^3 \left\{ 1 - 2 \left[\frac{1}{4\cos^2 \theta_W} \right] (c_v + \mathcal{P}_e c_a) + \left[\frac{1}{4\cos^2 \theta_W} \right]^2 (c_v^2 + c_a^2) (1 + \mathcal{P}_e A_e) \right\} \quad (6)$$

$$3. e^+e^- \rightarrow P^0\gamma:$$

$$\sigma = \frac{\alpha N_{tc}^2}{24\pi^3} \frac{s}{F_{tc}^2} \bar{\beta}^3 \left\{ 1 + 2 \left[\frac{1 - 4\sin^2 \theta_W}{4\sin^2 2\theta_W} \right] (c_v + \mathcal{P}_e c_a) + \left[\frac{1 - 4\sin^2 \theta_W}{4\sin^2 2\theta_W} \right]^2 (c_v^2 + c_a^2) (1 + \mathcal{P}_e A_e) \right\} \quad (7)$$

$$4. e^+e^- \rightarrow P^{0'}\gamma:$$

$$\sigma = \frac{\alpha N_{tc}^2}{216\pi^3} \frac{s}{F_{tc}^2} \bar{\beta}^3 \left\{ 1 - 2 \left[\frac{1}{4\cos^2 \theta_W} \right] (c_v + \mathcal{P}_e c_a) + \left[\frac{1}{4\cos^2 \theta_W} \right]^2 (c_v^2 + c_a^2) (1 + \mathcal{P}_e A_e) \right\} \quad (8)$$

where $\bar{\beta}^3 = (1 - M_P^2/s)^3$ is the phase space factor for the production of a heavy scalar and a massless vector.

The numerical values of the cross sections and left-right production asymmetries are listed in Table II for $\sqrt{s} = 1$ TeV, $F_{tc} = 123$ GeV, and $N_{tc} = 3$. The cross sections for the colored states benefit from the large size of α_s and the large color factor for gluon final states. Note that the cross section for $P^0\gamma$ is suppressed at the Z^0 but becomes relatively large at higher energies where photon exchange becomes significant (which is reflected in the small size of the left-right asymmetry).

Table II: The cross section (in point cross section units) and left-right production asymmetry for several PNGB-gauge-boson final states at $\sqrt{s} = 1$ TeV, $F_{tc} = 123$ GeV, and $N_{tc} = 3$.

Final State	σ	A_{LR}
$P_8^0 g$	$0.3 \cdot \bar{\beta}^3$	+0.65
$P_8^{0'} g$	$0.025 \cdot \bar{\beta}^3$	-0.60
$P_8^0 \gamma$	$0.006 \cdot \bar{\beta}^3$	+0.05
$P_8^{0'} \gamma$	$0.0008 \cdot \bar{\beta}^3$	-0.60

B. Signatures and Backgrounds

As in the case of the charged states, the branching ratios of the neutral PNGBs are, in general, model- and parameter-dependent. Nevertheless, in most models, heavy PNGBs decay into the heaviest fermions that are kinematically allowed. The signatures for the single production of neutral PNGBs are therefore

$$\begin{aligned} e^+e^- \rightarrow P_8^0 g &\rightarrow t\bar{t}g \rightarrow b\bar{b}W^+W^-g \quad M_P > 2m_t \\ &\rightarrow b\bar{b}g \quad M_P < 2m_t \\ e^+e^- \rightarrow P_8^{0'} \gamma &\rightarrow t\bar{t}\gamma \rightarrow b\bar{b}W^+W^-\gamma \quad M_P > 2m_t \\ &\rightarrow b\bar{b}\gamma \quad M_P < 2m_t \end{aligned} \quad (9)$$

where the gluons and photons are *monochromatic*. The dominant backgrounds to these signals, the Standard Model production of $Q\bar{Q}g$ and $Q\bar{Q}\gamma$ ($Q = t, b$), produce gluons and photons which have $1/k$ spectra. This difference is illustrated in Figure 2 which shows the measured gluon energy distribution that would be associated with the production of a 500 GeV P_8^0 . The sum of the signal and background distributions is shown as the solid histogram and the background distribution is shown as the dashed histogram.

The relatively high efficiency of b -tagging in the e^+e^- environment allows for a clean separation of the gluons from the b -jets in the P_8^0 (and $P_8^{0'}$) decays. To avoid confusion of the gluon with hadronic jets from the W decays, only leptonic W decays are considered in this study. The photons produced in association in color neutral PNGBs are distinguishable from all PNGB decay products and it is not necessary to employ b -tagging or to restrict the search to leptonic final states of the W 's.

Several other features help to distinguish PNGB production from the Standard Model backgrounds. Gluons (and photons) produced in association with neutral PNGBs are well-separated

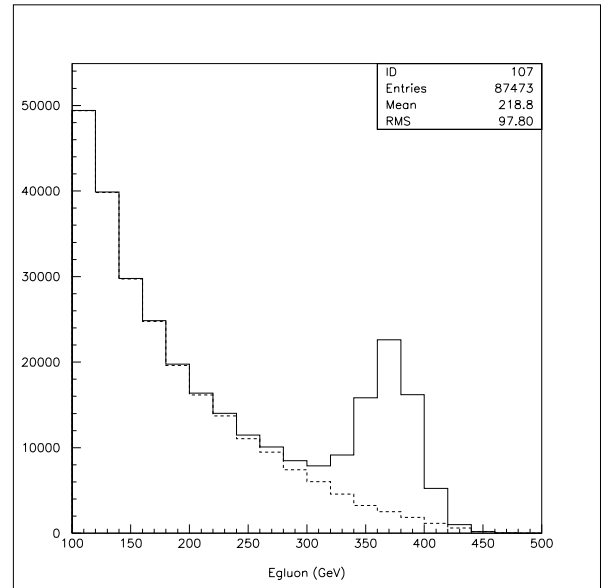


Figure 2: The measured gluon energy distribution in the process $e^+e^- \rightarrow t\bar{t}g$. The solid histogram shows the total distribution expected for a 500 GeV P_8^0 and the dashed histogram shows the MSM background.

spatially from the PNGB decay products whereas gluons produced in Standard Model $Q\bar{Q}$ production are radiated from internal and external quark lines and are spatially correlated with final state hadrons. The left-right asymmetry for the signal processes differs from the asymmetries associated with the background processes (0.34 for $t\bar{t}$ production and 0.62 for $b\bar{b}$ production). And finally, the spin correlations of the $t\bar{t}$ daughters of a PNGB differ from those of a $t\bar{t}$ pair produced by MSM processes and lead to small differences in the resulting $b\bar{b}$ joint energy distributions.

C. Discovery Limits

In order to assess the discovery potential of a TeV electron-positron collider for neutral PNGBs, a Monte Carlo simulation of the processes listed in equation 9 was performed. The simulation, which includes spin correlations in the $t\bar{t}$ decay chains, produces 4-vectors for final-state quarks, gluons, and leptons. The energies of these final state particles are smeared according to Gaussian resolution functions. Studies of the jet energy resolution of an NLC detector using a sophisticated reconstruction algorithm [3] indicate that it may be possible to achieve a resolution given by the following parameterization, $\sigma_{E_{jet}}/E_{jet} \simeq 0.34/\sqrt{E_{jet}}$. Since this is substantially better than any experiment has yet achieved, the simulated resolution was degraded by adding a 7% constant term in quadrature,

$$\frac{\sigma_{E_{jet}}}{E_{jet}} = \frac{0.34}{\sqrt{E_{jet}}} \oplus 0.07, \quad (10)$$

which is still twice the 14% energy resolution achieved by the UA2 Collaboration with an uncompensated calorimeter and without a magnetic spectrometer [9]. The results of this section are insensitive to this choice (the constant term can be varied substantially with essentially no change in results).

The backgrounds to the production of the color octet states are simulated using the ragTops (order- α_s) $t\bar{t}$ generator of Schmidt [10] and a simple, home-brewed $e^+e^- \rightarrow b\bar{b}g$ generator. The backgrounds affecting the color singlet search were simulated with a simple $e^+e^- \rightarrow Q\bar{Q}\gamma$ generator.

1. Color Octet States

The events produced by the $e^+e^- \rightarrow P_8^0 g$, $P_8^{0'} g$ and background simulations were selected according to the following selection criteria:

1. Three hadronic jets must be observed in the region of polar angle $|\cos\theta| < 0.95$.
2. (a) To search the region, $M_P > 2m_t$, two charged leptons must be observed in the region $|\cos\theta| < 0.95$.
(b) To search the region, $M_P < 2m_t$, the total energies of the observed jets must be larger than $0.6\sqrt{s}$ and the net transverse momentum of the three-jet system must be less than $0.1\sqrt{s}$.
3. The space angle between any two jets θ_{jj} must satisfy the following isolation criterion, $|\cos\theta_{jj}| < 0.90$.
4. Two of the hadronic jets were required to pass the b-tagging criteria.

In both search regions, the gluon was identified as the hadronic jet that did not satisfy the b-tagging criteria. In the region $M_P > 2m_t$, five quantities were determined for each selected event candidate: the gluon energy, the beam helicity (left-handed or right-handed), the space angle formed between the gluon and nearest b -jet, and the b -jet energies in the center-of-mass frame of the system recoiling against the gluon. For the region $M_P < 2m_t$, only the first three of these quantities were used.

The PNGB simulation was used to generate the normalized distribution function $S(\vec{x})$ of the five or three variables (labeled as \vec{x}) and the number of accepted signal events N_s for several PNGB masses. Note that N_s is an implicit function of N_{tc}/F_{tc} , $N_s = N_s^0 (N_{tc}/F_{tc})^2 (123/3)^2$, where N_s^0 is the number of accepted events at the nominal values of F_{tc} (123 GeV) and N_{tc} (3). The background simulations were used to generate the normalized distribution function $B(\vec{x})$ and the number of accepted background events N_b . The distributions and event totals were used to estimate the sensitivity of the PNGB search at each value of M_P . The sensitivity was characterized in two ways:

1. Assuming that the PNGB is not present, the value of N_{tc} is determined such that the likelihood ratio of the PNGB-present-hypothesis to the PNGB-absent-hypothesis was 0.05. Defining the total distribution function $T(\vec{x}) = f_s S(\vec{x}) + (1 - f_s) B(\vec{x})$ where $f_s \equiv N_s/(N_s + N_b)$ is

the signal fraction, the likelihood ratio condition can be expressed as follows,

$$\prod_{i=1}^{N_b} \frac{T(\vec{x}_i)}{B(\vec{x}_i)} = \exp \left\{ N_b \int d^N x B(\vec{x}) \ln \left[\frac{T(\vec{x})}{B(\vec{x})} \right] \right\} = 0.05. \quad (11)$$

The solution of equation 11 yields a 95% confidence region in M_P - N_{tc} space.

2. Assuming that the PNGB is present, the value of N_{tc} is determined such that ratio of f_s [as determined from a likelihood fit to the $T(\vec{x})$] to its uncertainty σ_f is five. In detail, it is necessary to solve the following equation,

$$\frac{f_s}{\sigma_f} = \left[N_s f_s \int d^N x \frac{1}{T(\vec{x})} \left(\frac{dT}{df_s} \right)^2 \right]^{\frac{1}{2}} = 5, \quad (12)$$

to determine the expected 5-sigma discovery region in M_P - N_{tc} space.

The 95%-confidence regions in M_P - N_{tc} space for P_8^0 and $P_8^{0'}$ are shown as solid and dashed curves, respectively, in Figure 3. The 5-sigma discovery regions are shown as solid and dashed curves in Figure 4. Note that limits are discontinuous across the point $M_P = 2m_t$ (shown as vertical dotted lines) where the analysis technique changes. The value $N_{tc} = 3$ is shown as horizontal dotted lines. Limits for values of F_{tc} other than 123 GeV can be determined by appropriately scaling N_{tc} (the limits for F_{tc}' and N_{tc}' are given by the $N_{tc} = N_{tc}'(123 \text{ GeV}/F_{tc}')$ line in Figs. 3 and 4).

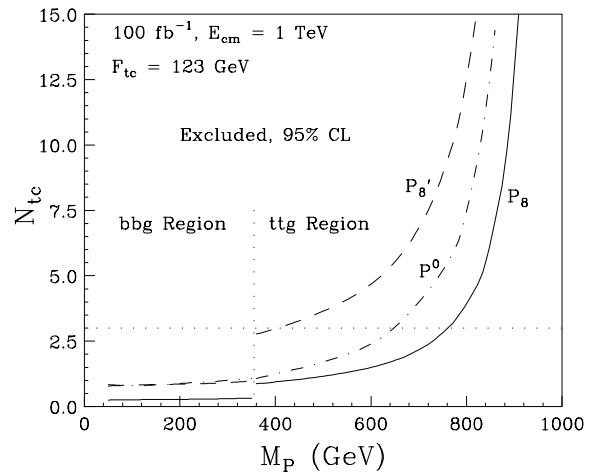


Figure 3: The 95% exclusion region in M_P - N_{tc} space for P_8^0 (solid curve), $P_8^{0'}$ (dashed curve), and P^0 (dashed-dotted curve).

It is clear that P_8^0 and $P_8^{0'}$ can be excluded or discovered for any realistic values of N_{tc} in the region $M_P < 2m_t$. In the region $M_P > 2m_t$, it is not possible to discover $P_8^{0'}$ with an analysis that uses only leptonic W decays unless N_{tc} is larger than

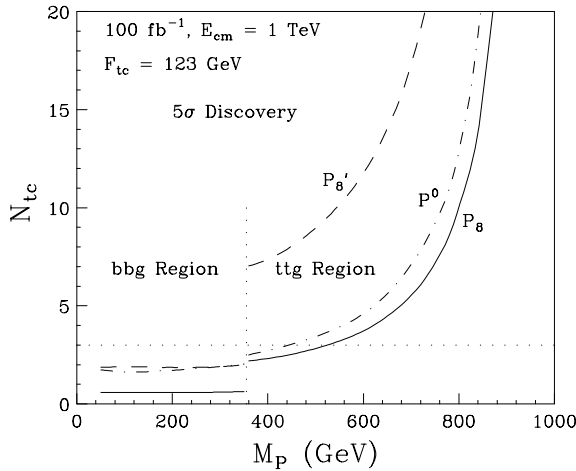


Figure 4: The 5-sigma discovery region in M_P - N_{tc} space for P_8^0 (solid curve), $P_8^{0\prime}$ (dashed curve), and P_8^0 (dashed-dotted curve).

7. Making the conservative assumption $N_{tc} = 3$, the $P_8^{0\prime}$ can be excluded at 95% confidence in the region $M_P < 404$ GeV. At $N_{tc} = 3$, the P_8^0 can be excluded at 95% confidence in the region $M_P < 761$ GeV and can be discovered at 5-sigma significance in the region $M_P < 524$ GeV.

2. Color Singlet States

The color singlet states P^0 and $P^{0\prime}$ are produced much less copiously than are the color octet states. However, they are associated with a fairly spectacular signature: an isolated, central, high energy (250-500 GeV), monochromatic photon recoiling against a hadronic or mixed hadronic-lepton system. Since the photon does not become confused with final state jets or leptons, it is not necessary to employ b -tagging or to require leptonic W decays. This helps to compensate for the small production rates and permits a useful search for P^0 . Unfortunately, the production rate for $P^{0\prime}$ is too small to be useful.

The events produced by the $e^+e^- \rightarrow P_8^0 \gamma$ and background simulations were selected according to the following selection criteria:

1. A photon must be observed in the region of polar angle $|\cos \theta| < 0.95$.
2. (a) To search the region, $M_P > 2m_t$, at least four hadronic jets or two jets and two charged leptons must be observed in the region $|\cos \theta| < 0.95$.
(b) To search the region, $M_P < 2m_t$, two hadronic jets must be observed in the region $|\cos \theta| < 0.95$. The total energies of the observed photon-jet system must be larger than $0.6\sqrt{s}$ and the net transverse momentum of the system must be less than $0.1\sqrt{s}$.
3. The space angle between the photon candidate and any jet or lepton $\theta_{\gamma j}$ must satisfy the following isolation criterion,

$$|\cos \theta_{\gamma j}| < 0.90.$$

For each accepted event, three quantities are determined: the photon energy, the beam helicity, the space angle formed between the photon and nearest jet or lepton. These quantities are used to generate signal and background distribution functions which are used to calculate 95% confidence and 5-sigma discovery regions in M_P - N_{tc} space as was done in section III.C.1. The regions are shown in Figures 3 and 4 as dashed-dotted curves. At $N_{tc} = 3$, the P^0 can be excluded at 95% confidence in the region $M_P < 646$ GeV and can be discovered at 5-sigma significance in the region $M_P < 452$ GeV.

IV. CONCLUSIONS

A high energy electron-positron collider is a useful device in the search for color singlet and octet pseudo-Nambu-Goldstone bosons. The search potential is summarized in Table III. Charged PNGBs can be discovered if their masses are less than $0.45-0.49\sqrt{s}$. The discovery reach for neutral states depends upon the ratio N_{tc}/F_{tc} . Three of the four neutral states can be discovered if their masses are less than 350-524 GeV even for the conservative parameter choice $N_{tc}/F_{tc} = 3/123$ GeV.

Table III: The 95%-exclusion and five-sigma discovery limits on the PNGB mass M_P are listed for a 1 TeV e^+e^- collider experiment with a 100 fb^{-1} integrated luminosity. The limits on the charge-neutral states are model-dependent and assume that $F_{tc} = 123$ GeV, and $N_{tc} = 3$.

PNGB	M_P Limit (95% CL)	M_P Limit (5- σ)
P_8^\pm	~ 500 GeV	490 GeV
P^\pm	~ 500 GeV	450 GeV
P_8^0	761 GeV	524 GeV
$P_8^{0\prime}$	404 GeV	350 GeV
P^0	646 GeV	452 GeV
$P^{0\prime}$	—	—

V. REFERENCES

- [1] C.J.S. Damerell and D.J. Jackson, *Vertex Detector Technology and Jet Flavor Identification at the Future e^+e^- Linear Collider* report at this workshop.
- [2] S. Chadha and M.E. Peskin, *Nucl. Phys.* **B185**, 61 (1981).
- [3] C.J.S. Damerell, *Ideas for the NLC Detector* report at this workshop.
- [4] A. Manohar and L. Randall, *Phys. Lett.* **B246**, 537 (1990).
- [5] L. Randall and E.H. Simmons, *Nucl. Phys.* **B380**, 3 (1992); G. Rupak and E.H. Simmons, *Phys. Lett.* **B362**, 155 (1995).
- [6] S. Dimopoulos, S. Raby, and G.L. Kane *Nucl. Phys.* **B182**, 77 (1981).
- [7] J. Ellis *et al.*, *Nucl. Phys.* **B182**, 529 (1981).
- [8] J. Kumar, M.E. Peskin, and M.L. Swartz, in preparation.
- [9] J. Alitti, *et al.*, *Z. Phys.* **C49**, 17 (1991).
- [10] C.R. Schmidt, *Phys. Rev.* **D54**, 3250 (1996).